

## INFLUENCE OF Al-Si LAYER TO STRUCTURE AND PROPERTIES ON INCONEL 713LC AND 738LC

Simona Pospíšilová

Tomáš Podrábský

Antonín Buchal

Brno University of Technology

Institut of Materials Science and Engineering

Technická 2896/2, 616 69 Brno

Czech Republic

### ABSTRACT

*This paper is focused on microstructure of protective layers created by co-deposition of Al and Si on nickel - base superalloys INCO 713 LC and INCO 738 LC after thermal and thermal-stress exposition and on microstructure of basic materials (substrates). The contribution also shows creep tests results for both superalloys with and without a protective layer.*

**Keywords:** Al-Si layer, creep test, INCO 713LC, INCO 738LC.

### 1. EXPERIMENTAL METHODS AND MATERIAL

A diffusion barrier from Al-Si layer was developed for turbine blades of aircraft engines from nickel-base superalloy ZhS6K as oxidation and corrosion protection. The main subject of the research is an application of Al-Si protect layers to alternative materials as are INCO 713LC and 738LC. A part of samples from the already mentioned superalloys were co - deposited by Al and Si and after that they were heat - treated. Another part of samples was kept without a layer. A chemical composition of individual melts from INCO 713LC and INCO 738LC is shown in table 1.

An operational degrading process was simulated by high-temperature heat treatment (temperature exposition) and by creep tests (temperature-stress exposition). The long-time annealing was performed in a kanthal furnace with normal atmosphere at temperatures from 700 to 1100°C for the duration from 50 to 1000 hours. The creep tests were run at temperatures from 750 to 1000°C (INCO 713 LC) and from 800 to 950°C (INCO 738 LC) under constant load without protect atmosphere.

*Table 1 Chemical composition of experimental material (at wt. %.)*

	C	Cr	Ti	Al	B	Zr	Nb	Ta	Mo	W	Co	Ni
INCO 713LC	0,05	12,08	0,75	5,91	0,010	0,10	2,02	< 0,05	4,58	-	< 0,05	Bal.
INCO 738LC	0,11	15,86	3,27	3,31	0,008	0,03	0,88	1,65	1,74	2,54	8,26	Bal.

### 2. RESULTS

#### 2.1. Creep test results

Due to comparison of creep-resistance, the coefficients  $A_4=20$  for both alloys INCO 713 LC and for INCO 738 LC were used. A graphical comparison of stress versus Larson-Miller parameter for the coated material by Al-Si layer and the uncoated material are shown in Fig. 1.

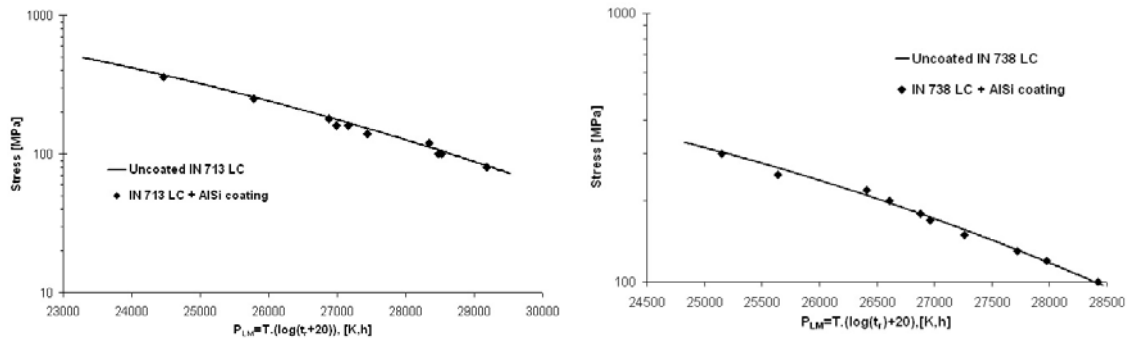


Figure 1. The influence of Al-Si layer to creep-resistance of INCO 713LC (on the left) and INCO 738LC (on the right)

## 2.2. Metallographic analysis of Al-Si layer

After co - deposition of Al and Si on the surface of material (Al+Si spray application and diffusion annealing at 950°C for 4 hrs), the main layer splits into several sub-layers. The light microscopy was performed by means of surface analysis (Fig.2, left). The uniformity, continuity of surface layers, thickness and structure of individual sub-layers were evaluated. Other methods of investigation were chemical analysis (EDS) of structure constituent and phases in layers (Fig.2, right).

According to the pictures and analyses from light and scanning electron microscopy, a split into several areas is evident. The surface of the samples from both materials at the initial state (without exposition) is divided into four sub-layers. The upper layer, called “oxide layer”, is very thin and discontinuous. By the spot and space analysis we detected  $\text{Al}_2\text{O}_3$  oxides which originated by diffusion from the layer, and under these oxides we can find  $\text{Cr}_2\text{O}_3$  which are created by diffusion from the base material. The second layer is a “coating zone” with Ni and Al phases. The next layer is called the “inter-diffusion zone” and contains more Si and heavy elements. Simultaneously the content of Ni and Al decreases. The last sub-layer, a “substrate diffusion zone”, is actually a band without  $\gamma'$  phase, sometimes with carbides with acicular morphology.

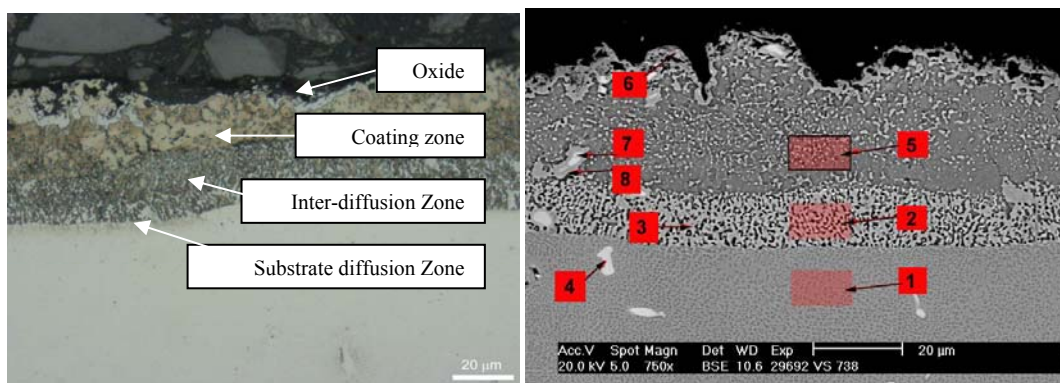


Figure 2. Microstructure of Al-Si layer, on the left - INCO 713LC, on the right – INCO 738LC, as received, marked areas on the right were analyzed by EDS.

Note: INCO 738LC, area 1 ( $\gamma + \gamma'$ ), area 2 (phases reached in Si, Mo, Cr, Co, W), area 3 (Cr-Si, Mo phase), area 4 (Nb, Ti, Ta complex carbide), area 5 (solid solution mixture and phases reached in Al), area 6 (Al, Cr oxide mixture), area 7 (Mo, Cr complex carbide), area 8 (Nb, Mo complex carbide).

After temperature and creep exposition, the thickness of particular layers is changed. Several sub-layers are created while several disappear. The distribution of single elements is also changed. From EDS microanalysis that followed, the oxygen stays on the surface and its content decreases with the distance from the surface. After temperature and creep exposition, the oxides  $\text{Al}_2\text{O}_3$  and  $\text{Cr}_2\text{O}_3$  are more created. After exposition at 1000°C and 200h, this layer is somewhere cracky and sporadically is a surface without layer. However, this temperature highly exceeds the working conditions. The surface of the samples without layer is non-uniform. There is a band without coherent  $\gamma'$ , depleted by Cr and Al and with titanium nitrides which have an acicular morphology. This band is extended with time and temperature. After thermal-stressed exposition cavities can occur.

### 2.3. Metallographic analysis of substrate

It also was observed microstructure of substrate on samples as received, after temperature (cross section) and creep exposition (cross and longitudinal section). The microstructure of nickel-base superalloys is changed by temperature and creep exposition. It comes to coarsening coherent  $\gamma'$  particles in matrix. This phase trends to unify and create the chain or block shapes with higher temperature. This process is not casual. It is evoked by chemical heterogeneity consequent upon segregation during the solidification. The morphology of the  $\gamma'$  particles, secreted into parallel plane by influence of temperature and stress, are termed as rafting [1]. The negative influence of this phenomenon is loss of coherence between  $\gamma'$  and  $\gamma$  phase. It also comes to growth of canals ( $\gamma$ ) between rafts and it causes soft movements of dislocations in grains or on grain boundary (2<sup>nd</sup> level of creep damage). The amount, size and shape of  $\gamma'$  phase in matrix can be observed by image analysis.

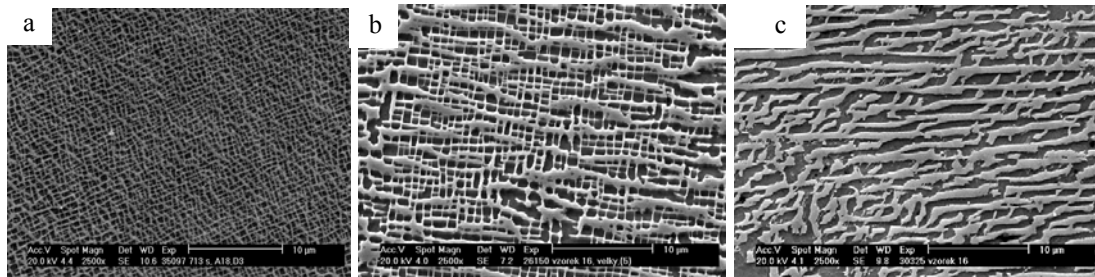
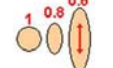
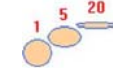


Fig.3 Microstructure of INCO 713LC, a) as received, b) after temperature exposition (950°C, 500h), c) after creep exposition (1000°C, 80MPa, 971h). Note:  $\gamma$  phase is light,  $\gamma'$  phase is dark.

The results from image analysis are shown in table 2. They clearly demonstrate an influence of temperature and creep exposition on phase  $\gamma'$  (morphology, quantity and size). It follows that area rate of  $\gamma'$  particles does not alternate with exposition, but morphology is changed ( $\gamma'$  coalescence and coarsening). An influence of cooperation of temperature and stress (creep exposition) is bigger than influence straight temperature. The same trends are illustrated on figure 3. The area amount of  $\gamma'$  particles is bigger in INCO 738LC, this material is heat treated from this point of view. It were estimated that Al-Si layer does not have an influence to quantity and morphology of particles  $\gamma'$ .

Table 2 Results of metallographic analysis by image analysis.

Specimen	$\gamma'$ phase [%]	$\gamma$ phase [%]	Sphericity 	Elongation 	Ratio max(b/a) 	Diameter [ $\mu$ m]		
						mean	max	min
713 VS0	46,58	53,42	0,48	1,63	1,49	0,35	0,4	0,27
713 VS1	48,74	51,26	0,48	1,69	1,53	0,53	0,61	0,36
713 T0 950°C, 500h	46,5	53,5	0,30	2,40	2,0	1,21	1,35	0,66
713 T1 950°C, 500h	47,5	52,5	0,29	2,30	2,25	1,22	1,37	0,78
713 TN0 1000°C, 80MPa, 971h	45,25	54,75	0,12	4,34	3,46	3,04	3,42	1,11
713 TN1 1000°C, 80MPa, 839h	48,2	51,8	0,11	4,19	3,22	3,00	3,5	0,9
738 VS0	65,42	34,58	0,44	1,73	1,56	0,41	0,48	0,30
738 VS1	65,48	34,52	0,47	1,61	1,49	0,50	0,56	0,37
738 T0 950°C, 500h	59,4	40,6	0,31	2,38	2,15	1,35	1,42	0,88

Note: VS(as received), T(temperature exposition),TN(creep exposition), 0(without layer), 1(with Al-Si layer)

### 2.4. Diffraction experiment

This is more exact approach than an image analysis because the measured area is all volume of specimen. Phase  $\gamma$  and  $\gamma'$  are coherent or semi-coherent and from this reason on the diffraction spectrum should be only one peak for both phases. It was estimated that the R-factor of  $\gamma'$  phase differs from  $\gamma$  phase and X-Ray diffraction was used.

Diffraction experiment was made on the X-Ray goniometer PW3050/10 in the equipment X'Pert fy. PHILIPS. Used was Bragg-Brentano configuration with  $\text{CoK}_\alpha$  radiation and proportional detector with crystal monochomator. Diffraction spectrum was measured in the step regime with step  $0.05^\circ 2\theta$

and delay 100 sec, in all positions. Diffraction record is shown on Fig.4, left. Experimental specimens were from INCO 713 LC, without layer and INCO 738LC with layer, both after creep exposition; samples were small and with very big grains. From this follows, the diffraction spectrum contains only one diffraction peak (311). But, this peak consists of two components, as is shown on Fig.4, right. We are assumed, that one component is from matrix, and the second component is from  $\gamma'$  phase (coherent to basic  $\gamma$  phase). The intensity of these components was separated and the individual intensity evaluated by the method of least squares. Ratio of these intensities indicated the content of  $\gamma'$  phase in superalloy. The results (table 3) are not exact, but it is the first estimate of content of precipitate  $\gamma'$ . Diffraction methods are not able to give better results for our specimen because the samples were small and with very big grains.

Table 3 Results of diffraction experiment, diffraction peak (311)

Specimen	$\gamma'$ phase [%]	$\gamma$ phase [%]	$R_\gamma$ [Å]	$R_{\gamma'}$ [Å]
713 TN0 800°C, 360MPa, 877h	56,8	43,2	43,86	36,94
738 TN1 850°C, 300MPa, 316h	62,3	37,7	46,98	36,94

Note:  $R_\alpha$ ,  $R_\beta$  is theoretical stray bulk (R-factor)

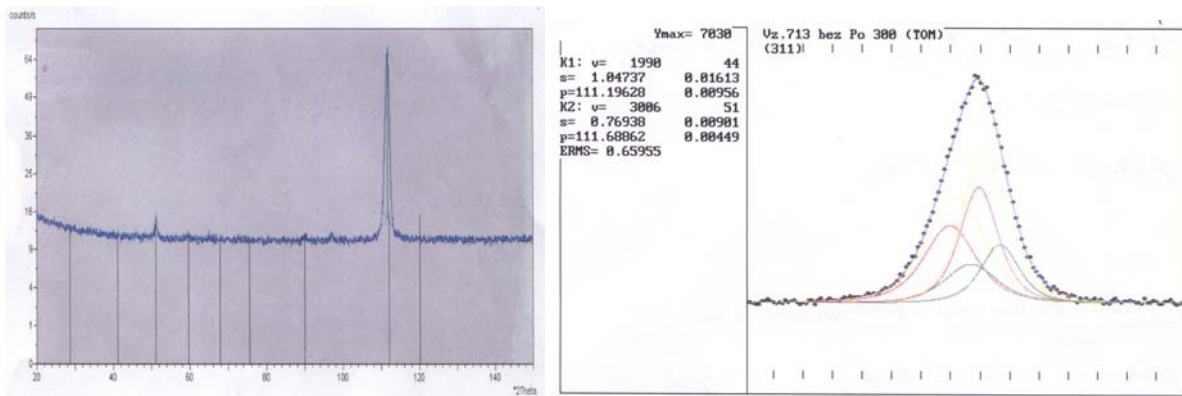


Fig.4 Results of diffraction experiment of INCO 713LC, without AlSi layer, after creep exposition (800°C, 360 MPa, 877h), on the left is diffraction record, on the right is diffraction double peak.

### 3. CONCLUSION

In the course of diffusion annealing of samples with Al-Si layer at temperatures from 700°C to 1100°C and after creep tests, intensive diffusion processes proceed. As a consequence, numerous phase transformations occur. The surface layer splits into several sub-layers called the oxide layer, coating zone, inter-diffusion zone and substrate diffusion zone. Owing to thermal and thermal-stress exposition, the coating zone and substrate diffusion zone expand. With increase of temperature (over 1000°C), the outstanding degradation is reached. A continuous layer containing Ni, Al, Cr, Si, Nb and Ti is created, and  $\gamma'$  precipitates also come to coagulation of.

By means of image analysis, there were estimated that with change of temperature and stress come to morphology modification of phase  $\gamma'$ . Total volume rate of  $\gamma'$  versus  $\gamma$  is not alternate. The results are almost same with comparison samples with and without protect layer. New method of X-Ray diffraction for volume rate of phase measurement was estimated.

*From the performed analyses follows that, the Al-Si layer improves heat-resistance of material and creep-resistance of materials INCO 713LC and 738LC is unchanged.*

*This research was supported by the Czech Science Foundation (Projects No. 106/07/1507 and 106/05/H008).*

### 4. REFERENCES

- [1] DURAND-CHARRE, M.: *The Microstructure of Superalloys*. Gordon & Breach Science Publishers, Amsterdam, 1997.